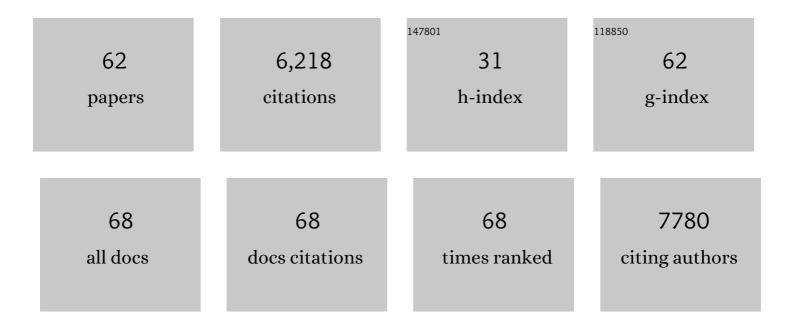
List of Publications by Year in descending order

Source: https://exaly.com/author-pdf/10566803/publications.pdf Version: 2024-02-01



Ηλο Ημλης

#	Article	IF	CITATIONS
1	Topochemical Synthesis of Copper Phosphide Nanoribbons for Flexible Optoelectronic Memristors (Adv. Funct. Mater. 14/2022). Advanced Functional Materials, 2022, 32, .	14.9	0
2	Gate-tunable linear magnetoresistance in molybdenum disulfide field-effect transistors with graphene insertion layer. Nano Research, 2021, 14, 1814-1818.	10.4	5
3	Hysteresis-free MoS <sub>2</sub> metal semiconductor field-effect transistors with van der Waals Schottky junction. Nanotechnology, 2021, 32, 135201.	2.6	9
4	Photothermal and Enhanced Photocatalytic Therapies Conduce to Synergistic Anticancer Phototherapy with Biodegradable Titanium Diselenide Nanosheets. Small, 2021, 17, e2103239.	10.0	13
5	Recent advances in the development of nanomedicines for the treatment of ischemic stroke. Bioactive Materials, 2021, 6, 2854-2869.	15.6	41
6	Van der Waals epitaxy of ultrathin crystalline PbTe nanosheets with high near-infrared photoelectric response. Nano Research, 2021, 14, 1955-1960.	10.4	19
7	Activating Carbon Nitride by BP@Ni for the Enhanced Photocatalytic Hydrogen Evolution and Selective Benzyl Alcohol Oxidation. ACS Applied Materials & Interfaces, 2021, 13, 50988-50995.	8.0	14
8	Transferred metal gate to 2D semiconductors for sub-1 V operation and near ideal subthreshold slope. Science Advances, 2021, 7, eabf8744.	10.3	37
9	From Octahedron Crystals to 2D Silicon Nanosheets: Facet elective Cleavage and Biophotonic Applications. Small, 2020, 16, e2003594.	10.0	11
10	Recent advances in long-term stable black phosphorus transistors. Nanoscale, 2020, 12, 20089-20099.	5.6	10
11	Intercalator-assisted plasma-liquid technology: an efficient exfoliation method for few-layer two-dimensional materials. Science China Materials, 2020, 63, 2079-2085.	6.3	5
12	Phaseâ€Changing Microcapsules Incorporated with Black Phosphorus for Efficient Solar Energy Storage. Advanced Science, 2020, 7, 2000602.	11.2	95
13	Black phosphorus field effect transistors stable in harsh conditions via surface engineering. Applied Physics Letters, 2020, 117, .	3.3	7
14	High Voltage Gain WSe <sub>2</sub> Complementary Compact Inverter With Buried Gate for Local Doping. IEEE Electron Device Letters, 2020, 41, 944-947.	3.9	14
15	Crystalline Red Phosphorus Nanoribbons: Large‣cale Synthesis and Electrochemical Nitrogen Fixation. Angewandte Chemie, 2020, 132, 14489-14493.	2.0	9
16	Crystalline Red Phosphorus Nanoribbons: Largeâ€6cale Synthesis and Electrochemical Nitrogen Fixation. Angewandte Chemie - International Edition, 2020, 59, 14383-14387.	13.8	58
17	Enhancing Performance of a GaAs/AlGaAs/GaAs Nanowire Photodetector Based on the Two-Dimensional Electron–Hole Tube Structure. Nano Letters, 2020, 20, 2654-2659.	9.1	106
18	Possible Luttinger liquid behavior of edge transport in monolayer transition metal dichalcogenide crystals. Nature Communications, 2020, 11, 659.	12.8	23

#	Article	IF	CITATIONS
19	Cladded Surface-Plasmon-Enhanced BP Photodetector Based on the Damage-Free Metal-Semiconductor Interface. IEEE Transactions on Electron Devices, 2020, , 1-4.	3.0	5
20	Highâ€Performance Photoinduced Memory with Ultrafast Charge Transfer Based on MoS <sub>2</sub> /SWCNTs Network Van Der Waals Heterostructure. Small, 2019, 15, e1804661.	10.0	42
21	Electrostatic Self-Assembly of Ti <sub>3</sub> C <sub>2</sub> T <sub><i>x</i></sub> MXene and Gold Nanorods as an Efficient Surface-Enhanced Raman Scattering Platform for Reliable and High-Sensitivity Determination of Organic Pollutants. ACS Sensors, 2019, 4, 2303-2310.	7.8	106
22	Inversion Symmetry Breaking Induced Valley Hall Effect in Multilayer WSe <sub>2</sub> . ACS Nano, 2019, 13, 9325-9331.	14.6	19
23	Comprehensive insights into effect of van der Waals contact on carbon nanotube network field-effect transistors. Applied Physics Letters, 2019, 115, .	3.3	4
24	Ultrasonic exfoliated ReS <sub>2</sub> nanosheets: fabrication and use as co-catalyst for enhancing photocatalytic efficiency of TiO <sub>2</sub> nanoparticles under sunlight. Nanotechnology, 2019, 30, 184001.	2.6	24
25	Template growth of Au/Ag nanocomposites on phosphorene for sensitive SERS detection of pesticides. Nanotechnology, 2019, 30, 275604.	2.6	15
26	Black Phosphorus: Thickness-Dependent Structural Stability and Anisotropy of Black Phosphorus (Adv. Electron. Mater. 3/2019). Advanced Electronic Materials, 2019, 5, 1970012.	5.1	2
27	Fluctuation of Volumetric Displacement in a Double Cell Vane Motor. , 2019, , .		Ο
28	Thicknessâ€Dependent Structural Stability and Anisotropy of Black Phosphorus. Advanced Electronic Materials, 2019, 5, 1800712.	5.1	11
29	A Low ost Metalâ€Free Photocatalyst Based on Black Phosphorus. Advanced Science, 2019, 6, 1801321.	11.2	79
30	Near-infrared light control of bone regeneration with biodegradable photothermal osteoimplant. Biomaterials, 2019, 193, 1-11.	11.4	181
31	Biodegradable near-infrared-photoresponsive shape memory implants based on black phosphorus nanofillers. Biomaterials, 2018, 164, 11-21.	11.4	94
32	Stable black phosphorus/Bi2O3 heterostructures for synergistic cancer radiotherapy. Biomaterials, 2018, 171, 12-22.	11.4	94
33	Plasmonic CuS nanodisk assembly based composite nanocapsules for NIR-laser-driven synergistic chemo-photothermal cancer therapy. Journal of Materials Chemistry B, 2018, 6, 1035-1043.	5.8	29
34	Inâ€Plane Black Phosphorus/Dicobalt Phosphide Heterostructure for Efficient Electrocatalysis. Angewandte Chemie - International Edition, 2018, 57, 2600-2604.	13.8	209
35	Near-infrared light-triggered drug delivery system based on black phosphorus for inÂvivo bone regeneration. Biomaterials, 2018, 179, 164-174.	11.4	115
36	Bismuth nanosheets as a Q-switcher for a mid-infrared erbium-doped SrF <sub>2</sub> laser. Photonics Research, 2018, 6, 762.	7.0	65

#	Article	IF	CITATIONS
37	Morphological control of gold nanorods via thermally driven bi-surfactant growth and application for detection of heavy metal ions. Nanotechnology, 2018, 29, 334001.	2.6	6
38	Different-sized black phosphorus nanosheets with good cytocompatibility and high photothermal performance. RSC Advances, 2017, 7, 14618-14624.	3.6	58
39	Efficient Enrichment and Self-Assembly of Hybrid Nanoparticles into Removable and Magnetic SERS Substrates for Sensitive Detection of Environmental Pollutants. ACS Applied Materials & Interfaces, 2017, 9, 7472-7480.	8.0	84
40	Controlled Patterning of Plasmonic Dimers by Using an Ultrathin Nanoporous Alumina Membrane as a Shadow Mask. ACS Applied Materials & Interfaces, 2017, 9, 36199-36205.	8.0	50
41	Synthesis of different-sized gold nanostars for Raman bioimaging and photothermal therapy in cancer nanotheranostics. Science China Chemistry, 2017, 60, 1219-1229.	8.2	49
42	Black phosphorus: a two-dimensional reductant for in situ nanofabrication. Npj 2D Materials and Applications, 2017, 1, .	7.9	63
43	Rücktitelbild: Surface Coordination of Black Phosphorus for Robust Air and Water Stability (Angew.) Tj ETQq1 I	0.78431 2.0	4 rgBT /Ov∈
44	Metabolizable Small Gold Nanorods: Size-dependent Cytotoxicity, Cell Uptake and <i>In Vivo</i> Biodistribution. ACS Biomaterials Science and Engineering, 2016, 2, 789-797.	5.2	51
45	Quantum Dots: Solvothermal Synthesis and Ultrafast Photonics of Black Phosphorus Quantum Dots (Advanced Optical Materials 8/2016). Advanced Optical Materials, 2016, 4, 1222-1222.	7.3	7
46	Biodegradable black phosphorus-based nanospheres for in vivo photothermal cancer therapy. Nature Communications, 2016, 7, 12967.	12.8	835
47	Solvothermal Synthesis and Ultrafast Photonics of Black Phosphorus Quantum Dots. Advanced Optical Materials, 2016, 4, 1223-1229.	7.3	326
48	Surface Coordination of Black Phosphorus for Robust Air and Water Stability. Angewandte Chemie, 2016, 128, 5087-5091.	2.0	116
49	Surface Coordination of Black Phosphorus for Robust Air and Water Stability. Angewandte Chemie - International Edition, 2016, 55, 5003-5007.	13.8	479
50	Small gold nanorods laden macrophages for enhanced tumor coverage in photothermal therapy. Biomaterials, 2016, 74, 144-154.	11.4	247
51	Ultrasmall Black Phosphorus Quantum Dots: Synthesis and Use as Photothermal Agents. Angewandte Chemie - International Edition, 2015, 54, 11526-11530.	13.8	906
52	Synthesis of gold/rare-earth-vanadate core/shell nanorods for integrating plasmon resonance and fluorescence. Nano Research, 2015, 8, 2548-2561.	10.4	43
53	Synthesis of bright upconversion submicrocrystals for high-contrast imaging of latent-fingerprints with cyanoacrylate fuming. RSC Advances, 2015, 5, 79525-79531.	3.6	42
54	Sensitive and Robust Colorimetric Sensing of Sulfide Anion by Plasmonic Nanosensors Based on Quick Crystal Growth. Plasmonics, 2014, 9, 11-16.	3.4	28

#	Article	IF	CITATIONS
55	Rose-bengal-conjugated gold nanorods for inÂvivo photodynamic and photothermal oral cancer therapies. Biomaterials, 2014, 35, 1954-1966.	11.4	276
56	Paper-based plasmonic platform for sensitive, noninvasive, and rapid cancer screening. Biosensors and Bioelectronics, 2014, 54, 128-134.	10.1	62
57	Synthesis of hollow rare-earth compound nanoparticles by a universal sacrificial template method. CrystEngComm, 2014, 16, 6141-6148.	2.6	29
58	Competitive Reaction Pathway for Siteâ€5elective Conjugation of Raman Dyes to Hotspots on Gold Nanorods for Greatly Enhanced SERS Performance. Small, 2014, 10, 4012-4019.	10.0	21
59	Bimodal optical diagnostics of oral cancer based on Rose Bengal conjugated gold nanorod platform. Biomaterials, 2013, 34, 4274-4283.	11.4	74
60	Near-infrared absorption imaging and processing technologies based on gold nanorods. Wuhan University Journal of Natural Sciences, 2013, 18, 307-312.	0.4	1
61	Topochemical Synthesis of Copper Phosphide Nanoribbons for Flexible Optoelectronic Memristors. Advanced Functional Materials, 0, , 2110900.	14.9	11
62	Strain Balanced Self‣upporting Singleâ€Crystalline LiNbO 3 Thin Films for Flexible Electronics. Advanced Electronic Materials, 0, , 2100986.	5.1	0